Asian Journal of Chemistry; Vol. 33, No. 5 (2021), 994-1000

ASIAN JOURNAL OF CHEMISTRY

https://doi.org/10.14233/ajchem.2021.23109

Interaction of Midazolam with Glassy Carbon Supported Lipid Membrane in the Presence and Absence of Marker Ions

M. PADMAPRIYA[1], K. PARVATHI[2] and S. RAMESHKUMAR[1,*]

[1]Department of Chemistry, Sri Vasavi College, Erode-638316, India
[2]Department of Chemistry, L.R.G. Government Arts College for Women, Tirupur-641604, India

*Corresponding author: E-mail: srksvc2016@gmail.com

Received: 28 December 2020; *Accepted*: 16 February 2021; *Published online*: 16 April 2021; AJC-20316

A biomimetic membrane was formed on the surface of electrochemically activated glassy carbon electrode in NaCl bath solutions. The variation of electrochemical properties of solid supported bilayer lipid membrane (s-BLM) with NaCl concentration in the bath solutions in the presence and absence of ferri/ferrocyanide marker ions was discussed using electrochemical impedance spectroscopy. The extent of pore formation on the s-BLM surface was discussed using bode phase diagram. The electrochemical impedance studies show that the partition of midazolam into the s-BLM strongly depends on Cl^- ion concentration in the bath solutions. The variation of membrane capacitance with drug dose shows the ionized form of midazolam interaction with the surface of s-BLM while the neutral and ion pair forms get partitioned into the membrane. In the presence of marker ions, the membrane resistance increases with decrease in NaCl concentration in the bath solution. The cyclic voltammetric responses of marker ions for bare and drug doped s-BLMs in NaCl bath solutions were recorded and variation of redox peak currents with drug dose was discussed.

Keywords: Glassy carbon electrode, Solid supported bilayer lipid membrane, Cyclic voltammetry, Drug-membrane interaction.

INTRODUCTION

Biomembranes are important components of all living organisms forming a boundary between or within cells and cell organelles [1]. The phospholipid molecules, self assembled into a bilayer, serve as a major component of a biomembrane and a basic matrix for other constituents of biomembranes, namely, protein and carbohydrate [1]. In order to understand various biological processes taking place at the membrane-electrolyte interface and across the biomembrane some model membrane systems have been developed. The model membrane systems have played an important role in identifying and understanding the properties of biomembranes [2]. The biomimetic membrane systems include vesicles [3], bilayer lipid membranes (BLMs) [4] and solid supported bilayer lipid membranes (s-BLMs) [5]. s-BLMs are more robust and stable than planar bilayer lipid membranes and can be easily deposited on a variety of hydrophilic surfaces such as oxidized glassy carbon electrode [6]. The solid supported bilayer lipid membranes have many advantages in addition to above, such as ease and reproducibility of preparation, long-term stability, electrochemical detective ability [7]. This type of membrane systems can be extensively used for studying the interaction of some biomolecules and drug molecules with supported bilayer lipid membranes [8-10].

Benzodiazepines are a group of neuroactive drugs widely used for their hypnotic, muscle relaxant, anxiolytic and anti-convulsant properties [11-13]. The pharmarcological actions of benzodiazepines are due to their binding to the specific sites in membrane bound proteins and the lipid background is considered to play a more passive role [14-16]. Midazolam, belongs to benzodiazepine, is used as a short-acting sleep inducing agent for sedation for short procedures, induction of an anesthesia and prolonged sedation in intensive care units [13]. Being lipophilic, midazolam also interacts non-specifically with biomembranes and reach concentrations one order of magnitude higher than that in surrounding medium [17,18], affecting membrane structural properties [19-21]. This type of non-specific interactions may mediate several effects of midazolam observed at global concentrations above its affinity for specific receptors, such as some anticonvulsant actions [22,23] and inhibitor action for calcium-calmodulin dependent protein kinase [24], voltage sensitive Ca^{2+} channels [25] and Na^+ channels [26].

Few analytical methods have been reported for the assay of midazolam in pharmaceutical formulations and biological matrices [13]. Polarographic and voltammetric methods have also been developed for the determination of midazolam in pharmaceutical formulation in organic solvents [27-29]. Literature survey reveals that only one electroanalytical method was reported for assay of midazolam using surfactants [1]. However, the fact that at pH > 4, an additional ring in midazolam undergoes ring opening was not considered and the voltammetric responses were misinterpreted and the research works on the detection of midazolam at lower concentrations is almost scanty. Hence, the present study aimed to study the interaction of midazolam with solid supported bilayer lipid membrane (s-BLM) and to develop an electrochemical sensor using ferri/ferrocyanide marker ions.

EXPERIMENTAL

The hydrochloride salt of midazolam ($MDZH^+Cl^-$) obtained from Neon Laboratories Ltd., India was used for the studies. A stock solution of egg lecithin containing greater than or equal to 99% L-α-phosphatidylcholine (Sigma-Aldrich) was prepared by disso-lving (5 mg/mL) in chloroform. The bilayer lipid membrane (BLM) forming dispersion was prepared by evaporating 100 µL of the stock solution in a 2 mL screw-cap tube under nitrogen atmosphere and dissolving the resulting lipid film in 200 µL of *n*-decane (Merck, Germany).

All other reagents ($K_4[Fe(CN)_6]$, $K_3[Fe(CN)_6]$, $NaHCO_3$, NaCl, chloroform, *n*-decane, *etc.*) were of analytical grade and water used for preparation of solutions was purified by ion exchangers and filtered by a Millipore Milli-Q-system (R > 18 MΩ cm^{-1} at 25 ºC).

The glassy carbon electrode of diameter 2 mm was used as a solid support for bilayer lipid membrane. Before membrane formation the electrode surface was polished with alumina slurry using polishing kit, washed with double distilled water and activated electrochemically by cyclic voltammetric method using the procedure described by Devadas *et al.* [30]. All electrochemical experiments were performed with a potentiostat, GAMRY REFERENCE 600, using a three electrode set up. The BLM coated GCE electrode served as working electrode, Ag/AgCl electrode served as reference electrode and a Pt foil was used as counter electrode. The electrochemical studies were carried out at room temperature (25 ± 1 ºC). Stirring device, vibration isolated platform, Faraday cage and Ag/AgCl electrodes were fabricated following standard procedures [31-35]. The formation of BLM on GCE surface, its electrochemical characterization, subsequent interaction with midazolam in 1.0 M, 0.1 M and 0.01 M NaCl bath solutions containing 1 mM $Fe(CN)_6^{3-/4-}$ had been done using electrochemical impedance spectroscopic and cyclic voltammetric methods. The electrochemical impedance spectra were recorded at open circuit potential by superimposing a sinusoidal AC signal of small amplitude 25 mV in the frequency range 1 MHz to 10 mHz. Analysis of the impedance data was done using Gamry Echem Analyst software. The pH of the bath solutions was maintained 7 using Britton-Robinson (B-R) buffer, prepared by mixing after every drug dose, a stabilization period of 30 min was allowed for the drug to equilibrate between the two phases. A lipid solution in *n*-decane (3 µL) was applied on the electrochemically activated surface of GCE and allowed to dry under nitrogen atmosphere. Again, 3 µL of lipid solution was applied and immersed in 3.5 mL NaCl bath solution for 30 min, where the L-α-phosphatidylcholine molecules underwent self assembly to form the lipid bilayer and the electrical impedance |z| and phase angle remained almost stable for 38 h in most of the experiments. The experiments were carried out five times to check the reproducibility and the relative difference between replica experiments was found to be less than 3% at room temperature, which shows good reproducibility.

RESULTS AND DISCUSSION

Electrochemical activation of GCE and formation of BLM on GCE surface: The surface of GCE was activated in 0.1 M $NaHCO_3$ solution by using cyclic voltammetric technique. The well polished glassy carbon electrode was taken in 0.1 M $NaHCO_3$ solution, after placing Ag/AgCl (reference electrode) and a Pt foil (counter electrode), the cyclic voltammograms were recorded in the potential range –0.8 to 1.6 V at the scan rate 100 mV/s. The cyclic voltammograms of GCE activation is shown in Fig. 1. The formation of highly porous, highly reactive oxygen containing functional groups and oxidized carbon on the GCE surface is related to the anodic peak observed around 1 V [36]. This anodic peak current doesn't increase significantly up to 10 cycles and starts to increase from 10th cycle, reaching a maximum current at 21st cycle (inset Fig. 1). Hence, before applying BLM forming solution on GCE, it was electrochemically activated by cyclic voltammetry (minimum 20 cycles). The surface of GCE was highly porous, rough and highly electrochemically active compared to that of bare GCE. 3 µL of L-α-Phosphatidylcholine in *n*-decane was applied on dry electrochemically activated GCE surface using a micro syringe and immediately immersed in the NaCl bath solution, whereupon, the bilayer lipid membrane formed spontaneously. The electrical properties of s-BLM are stable after 30 min, indicating a stable membrane was formed on GCE surface.

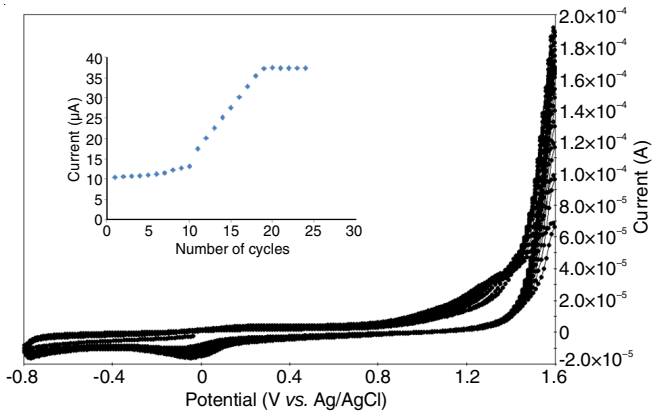

Fig. 1. Electrochemical activation of GCE

Electrochemical impedance studies (EIS): The formation of s-BLM on the surface of electrochemically activated GCE was monitored by EIS. After applying 3 µL of L-α-phosphati-

dylcholine in *n*-decane on the dry surface of electrochemically activated GCE, the GCE was immediately immersed in the respective NaCl bath solutions at neutral pH (B-R buffer) for 30 min. Fig. 2 shows the Nyquist plots of BLM coated GCE in 1.0 M, 0.1 M and 0.01 M NaCl bath solutions, respectively. The Nyquist plots obtained are not straight-forward and analysis of the impedance spectra is done using an equivalent circuit [37]. An equivalent circuit is constructed using resistors, capacitor and Warburg impedance to represent the dominant components of biomimetic membrane. The experimental curves obtained fit well with the equivalent circuit [37] shown in Fig. 3, where R_s is solution resistance, C_M is membrane capacitance, R_M is membrane resistance and W is Warburg resistance which represents mass transfer.

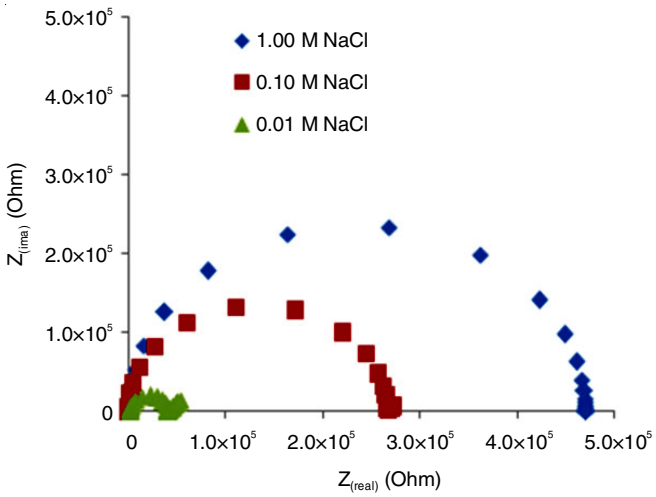

Fig. 2. Nyquist plots of BLM formed on electrochemically activated GCE surface in NaCl bath solutions

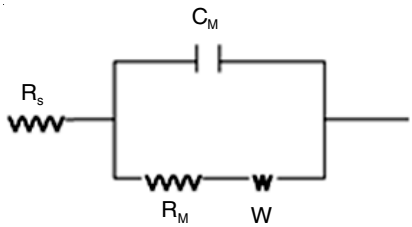

Fig. 3. Equivalent for BLM formed on electrochemically activated GCE surface

Under AC conditions, the frequency domains in which these circuit elements, corresponding to different parts of membrane, dominate can be identified when their resistances differ too. The rule is such that when the circuit elements are in series, the total resistance of the circuit is determined by the circuit element with the highest resistance and by the lowest resistance of the circuit element when they are connected parallel [38,39]. The contribution from a pure resistor to the total impedance is independent of AC frequency, while the contribution of pure capacitor to the total impedance is frequency dependent and is given as:

$$X_C = \frac{1}{\omega C} = \frac{1}{2\pi f C} \quad (1)$$

where, f is AC frequency and C is capacitance of a capacitor.

At the highest frequencies $1/\omega C_M$ is smaller than both R_S and R_M, hence from the above mentioned rule the overall impedance |Z| is determined by the solution resistance R_s. With decrease in frequency the value of $1/\omega C_M$ increases and becomes greater than R_s, but still smaller than R_M. Now in these frequencies the overall impedance is determined by $1/\omega C_M$. This is characterized by a straight line with a slope –1 in the plot of |Z| *vs*. log f (Fig. 4). With further decrease in frequency $1/\omega C_M$ increases and becomes greater than R_M, now the overall impedance is dominated by R_M, which is shown by a parallel line to frequency axis. The formation of BLM on electrochemically activated GCE was confirmed by calculating thickness of BLM employing the equation:

$$d = \frac{A\varepsilon\varepsilon_0}{C_M} \quad (2)$$

where A is area of BLM, ε is dielectric constant of lipid bilayer, which is 2.05 [40]; ε_0 is permittivity of free space ($\varepsilon_0 = 8.854 \times 10^{-12}$ Fcm^{-1}); C_M is capacitance of lipid bilayer phase.

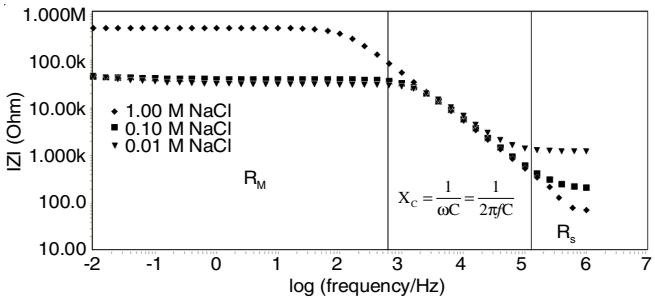

Fig. 4. Bode impedance plots of BLM formed on electrochemically activated GCE surface

The thickness of BLM formed on GCE was calculated to be 4.9, 5.3 and 5.92 nm, respectively in 1.0 M, 0.1 M and 0.01 M NaCl bath solutions. These values are very close to twice the thickness of monolecithin layer (2.5 nm) [39-42]. The electrochemical parameters derived using the equivalent circuit are represented in Table-1. It is clear that the thickness of s-BLM increases and capacitance decreases with decrease in NaCl concentration in the bath solution.

TABLE-1
VARIATION OF CAPACITANCE AND THICKNESS OF BLM WITH THE CHANGE IN BATH CONCENTRATION

Concentration of NaCl in the bath solution (M)	Capacitance of lipid bilayer (C_M) × 10^{-9} F	Resistance of lipid bilayer membrane (R_M) kΩ
1.00	2.93	471
0.10	2. 71	39.2
0.01	2.43	32.5

The surface positive charge (due to nitrogen bases) on the BLM was mostly neutralized by Cl^- ions from the bath solution and the surface is negatively charged due to unneutralized negative charges (phosphate group). These negative charges are partially neutralized by adsorption of Na^+ ions from bath solution [38,43]. When the NaCl concentration increases in

the bath solution, the adsorption of both Na^+ and Cl^- ions on the BLM surface increases. The adsorbed ions show tightening effect on the BLM surface and reduce its thickness, which is inversely proportional to its capacitance. Hence, membrane capacitance increases with increase in NaCl concentration in the bath solution. From Table-1, it can also be seen that the membrane resistance decreases with decrease in NaCl concentration in the bath solution. Though BLM is impermeable to most of the ions and larger molecules, it is leaky to smaller ions such as Na^+ and K^+ through the minute pores [44].

When the positive charges on the BLM surface are mostly neutralized by Cl^- ions, most of the pores on the BLM surface are highly covered and there is more resistance for flow of smaller ions across lipid bilayer. Hence, BLM resistance increases with increase in extent of Cl^- ion adsorption *i.e.* NaCl concentration in the bath solution. With decrease in NaCl concentration, the sizes of pores on the BLM surface increases and membrane resistance decreases. The deviation of phase angle from 90º and decrease in frequency domain nearly at 90º, corresponding to capacitive region (Fig. 5) shows increase in size of pores in the BLM surface [45].

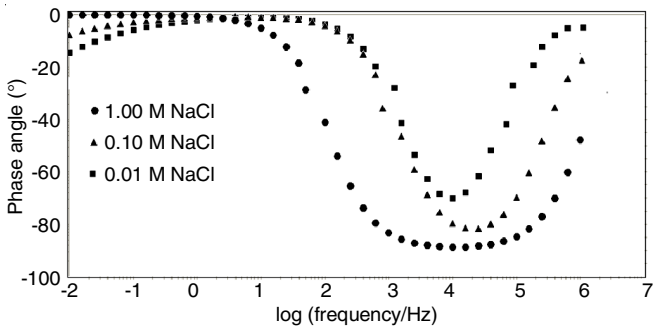

Fig. 5. Bode phase diagrams of BLM formed on electrochemically activated GCE surface

After forming BLM on electrochemically activated GCE surface, the s-BLM was immersed in respective NaCl bath solutions containing 1:1 ratio 1 mM $Fe(CN)_6^{3-/4-}$ ions. The impedance spectra for bare and drug doped s-BLMs are shown in Fig. 6a-c. From these plots, it is clear that in the presence of $Fe(CN)_6^{3-/4-}$ ions, the membrane resistance increases with decrease in NaCl concentration in the bath solution, which is an opposite trend observed in the absence of $Fe(CN)_6^{3-/4-}$ ions. Moreover, the deviation of phase angle from 90º (Fig. 7) with NaCl concentration in the bath solution followed same trend as observed in the absence of $Fe(CN)_6^{3-/4-}$ ions. This indicates that in presence of $Fe(CN)_6^{3-/4-}$ ions in the NaCl bath solutions, the pore sizes are not greatly affected. The decreasing trend of membrane resistance with decrease in NaCl concentration in the bath solution is retained when s-BLM is again placed in respective NaCl bath solutions (in absence of $Fe(CN)_6^{3-/4-}$ ions) in 30 min and the electrical properties measured again are very close to the values measured initially formed in the NaCl bath solutions.

Recent research works [46-48] on biosensor applications of s-BLM indicated that $Fe(CN)_6^{3-/4-}$ ions can enter into lipid bilayer phase and reach the GCE surface. When $Fe(CN)_6^{3-/4-}$ ions pass through the lipid bilayer phase, there will be an electrostatic attractive force between $Fe(CN)_6^{3-/4-}$ and Na^+ ions passing through the membrane, which will reduce the mobility of Na^+ ions across lipid bilayer phase and increases the membrane resistance. When the size of pores on the BLM surface increases the penetration of $Fe(CN)_6^{3-/4-}$ ions into the BLM phase also increases and the extent of electrostatic interaction between Na^+ ions and $Fe(CN)_6^{3-/4-}$ ions also increases. This electrostatic attraction greatly reduce the mobility of Na^+ ions in the BLM phase and thereby increases its resistance. This could be reason for increase in membrane resistance with decrease in NaCl concentration in the bath solution in the presence of $Fe(CN)_6^{3-/4-}$ ions.

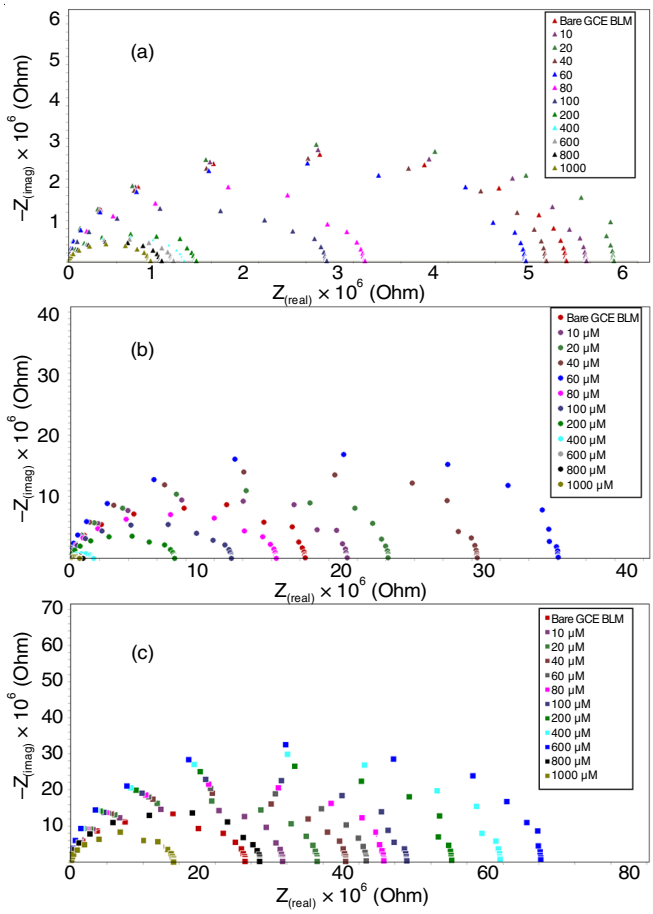

Fig. 6. Nyquist plots of bare and drug doped s-BLMs in 1.0 M, 0.1 M and 0.01 M NaCl bath solutions in the presence of 1 mM $Fe(CN)_6^{3-/4-}$ ions

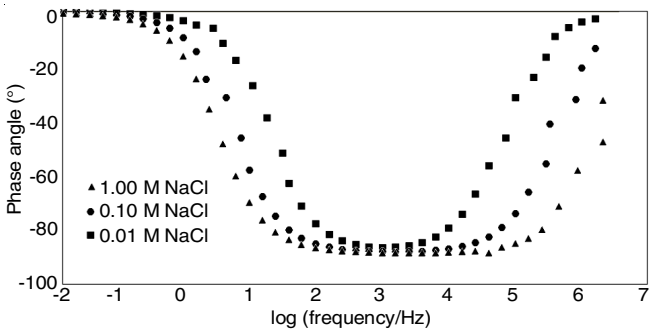

Fig. 7. Bode phase diagram of s-BLMs in the presence of 1 mM $Fe(CN)_6^{3-/4-}$ ions in NaCl bath solutions

The Nyquist plots obtained for bare and drug doped s-BLMs in the presence of marker ions $Fe(CN)_6^{3-/4-}$ in the NaCl bath solutions fitted well with the equivalent circuit shown in Fig. 3. The corresponding electrochemical impedance parameters are shown in Table-2. From Table-2, it is clear that the membrane resistance increases initially and then starts to decrease beyond certain concentration in the NaCl bath solutions. In solution midazolam exists neutral, ionized and ion pair forms. The equilibrium between different species in solution can be represented by the following equation [38,49]:

$$MDZH^+Cl^-_{(solution)} \rightleftharpoons MDZH^+_{(aq)} + Cl^-_{(aq)} \rightleftharpoons [MDZH^+..Cl^-]_{(ion\text{-}pair)} \quad (3)$$

The extent of these forms in solution is strongly influenced by NaCl concentration. Due to common ion effect of Cl^- ion the ionized form will exist in lower proportion in 1.0 M NaCl bath solution than in 0.1 M and 0.01 M NaCl bath solutions. The ionized form exists in larger amount in 0.01 M NaCl bath solutions. The positively charged ($MDZH^+$) species obtained from ionization of midazolam gets attached to the unneutralized negative charges on the BLM surface BLM electrostatically [38]. The extent of this interaction is larger in 0.01 M NaCl bath solution than that in 1.0 M and 0.1 M NaCl bath solutions, due to more negative charge on BLM surface as explained earlier and large amount of ionized form of midazolam in 0.01 M NaCl bath solution. The electrostatic interaction of ionized form of midazolam with BLM surface further reduces the pore sizes and thereby offers more resistance for the flow of Na^+ ions and hence the membrane resistance increases. Midazolam starts to get partitioned into the membrane when neutral and ion pair forms are formed in the bath solution. The partition of midazolam into the BLM fluidizes it and makes the BLM much leakier to smaller ions like Na^+ and K^+.

The variation of membrane capacitance with drug dose (Fig. 8) shows that the membrane capacitance (C_M) increases with drug dose and is biphasic in nature. The initial increase in membrane capacitance is due to the tightening the effect shown by ionized midazolam and the second phase increase in capacitance is due to the partition of midazolam into the membrane [38], which increases the membrane area.

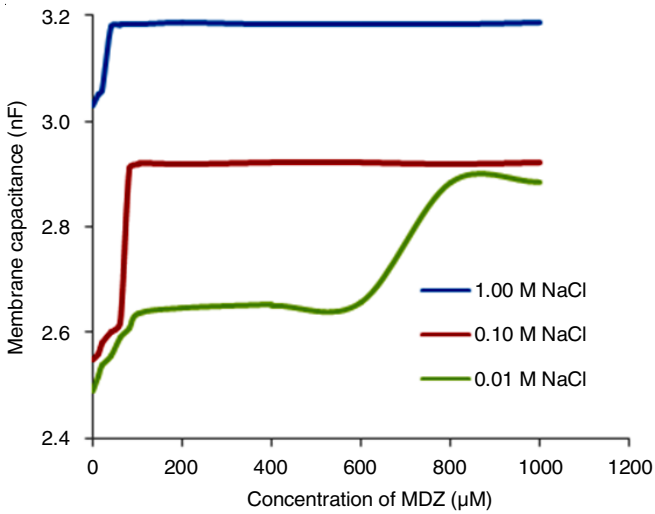

Fig. 8. Variation of membrane capacitance with drug dose in the presence of 1 mM $Fe(CN)_6^{3-/4-}$ ions

Voltammetric studies: Fig. 9a-c show the cyclic voltammograms electrochemically activated bare GCE and BLM coated GCE in 1.0 M, 0.1 M and 0.01 M NaCl bath solutions respectively in the presence of 1:1 ratio 1 mM $Fe(CN)_6^{3-/4-}$ ions. Before studying cyclic voltammograms, the BLM forming solution was applied on the GCE surface and immersed in the respective NaCl bath solutions for 30 min, where the self assembly of L-α-phosphatidylcholine molecules into a bilayer on GCE surface will be complete. Then the BLM coated GCE was transferred into respective NaCl bath solutions containing 1:1 ratio of 1 mM $Fe(CN)_6^{3-/4-}$ ions and the cyclic voltammograms were recorded. From the cyclic voltammograms, it is clear that when GCE was coated with BLM, a decrease of peak current and a slight increase of peak to peak-to-peak separation between cathodic and anodic waves was observed. Thus, it could be concluded that the electronic communication of $Fe(CN)_6^{3-/4-}$ ions to the GCE surface had been inhibited by BLM to a certain degree [7]. This indicated the formation of s-BLM on GCE surface. The peak-to-peak separation increases with decrease in NaCl concentration in the bath solution and is very large in 0.01 M NaCl bath solution. Further, both anodic

TABLE-2
ELECTROCHEMICAL IMPEDANCE PARAMETERS OF BLM FORMED ON ELECTROCHEMICALLY ACTIVATED GCE SURFACE IN NaCl BATH SOLUTIONS

Concentration of MDZ (μM)	1.0 M NaCl Bath solution		0.1 M NaCl Bath solution		0.01 M NaCl Bath solution	
	$C_M \times 10^{-9}$ F	R_M MΩ	$C_M \times 10^{-9}$ F	R_M MΩ	$C_M \times 10^{-9}$ F	R_M MΩ
0	3.030	52.15	2.550	16.35	2.490	24.17
10	3.050	53.02	2.560	19.27	2.520	29.41
20	3.060	53.22	2.580	22.16	2.540	34.20
40	3.180	5.030	2.604	28.37	2.558	38.16
60	3.182	4.81	2.620	34.04	2.592	41.01
80	3.184	3.11	2.911	14.32	2.610	43.44
100	3.183	2.71	2.920	11.21	2.638	46.61
200	3.186	1.33	2.919	7.23	2.647	52.84
400	3.184	1.27	2.922	1.58	2.653	59.61
600	3.185	1.09	2.922	0.988	2.659	65.26
800	3.184	0.965	2.919	0.813	2.885	26.22
1000	3.186	0.849	2.921	0.571	2.886	14.86

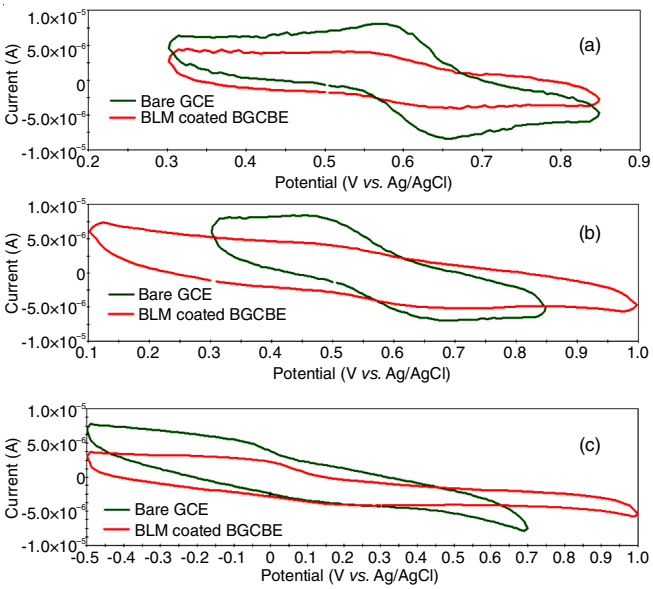

Fig. 9. Cyclic voltammetric response of bare and BLM coated GCEs in 1.0 M,0.1 M and 0.01 M NaCl bath solutions respectively, containing 1:1 ratio of 1 mM of $Fe(CN)_6^{3-/4-}$ ions

and cathodic peaks are shifted in the negative direction with decrease in NaCl concentration in the bath solution. While running cyclic voltammogram NaCl electrolyte acts as supporting electrolyte and when its concentration decreases the contribution from double layer charging current increases, where most of the ions arrange parallel to the charged electrode surface rather than undergoing redox reactions.

Cyclic voltammetry studies: Cyclic voltammograms were recorded in the presence and absence of midazolam at various doses in 1.0 M, 0.1 M and 0.01 M NaCl bath solutions containing 1:1 ratio of 1 mM $Fe(CN)_6^{3-/4-}$ ions. It was observed that the cyclic voltammetry responses for the electrochemical redox reactions do not show a continuous increase in peak current in 1.0 M NaCl bath solution with drug dose. In this bath solution, the surface coverage by Cl^- ions is relatively larger than that in 0.1 M and 0.01 M NaCl bath solutions and hence the pore size on the BLM surface is relatively smaller as discussed earlier. Therefore, the penetration of $Fe(CN)_6^{3-/4-}$ ions into s-BLM is difficult. In 0.01 M NaCl bath solution, the contribution from charging current is larger and cyclic voltammetric responses didn't show a definite trend in peak currents in the presence of midazolam. However, in 0.1 M NaCl bath solution the peak current increased with drug dose is shown in Fig. 10. The variation of redox peak currents of $Fe(CN)_6^{3-/4-}$ ions with drug dose in 0.1 M NaCl bath solution at s-BLM surface shows the variation of redox peak currents with drug dose is biphasic (Fig. 11). This is similar to the results obtained for interaction of surfactin with supported s-BLM [7].

The initial increase in peak currents, which is linear with drug dose upto 60 µM, is due to the interaction of ionized form of midazolam, which gets attached to the s-BLM surface and offers some resistance to the penetration of $Fe(CN)_6^{3-/4-}$ ions. A second phase increase in peak currents was observed from 80 µM midazolam concentration, *i.e.* when midazolam is partitioned into the s-BLM. The second phase increase in peak

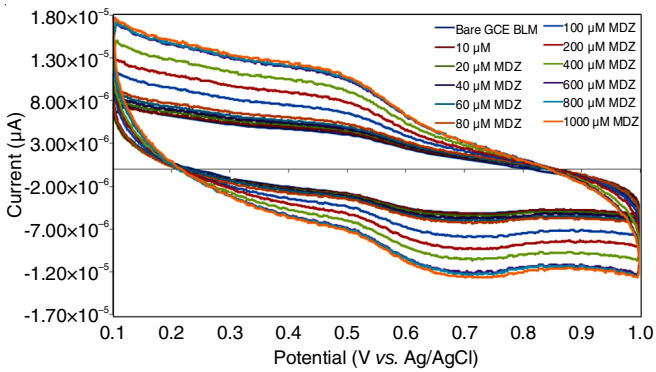

Fig. 10. Cyclic voltammetric response of $Fe(CN)_6^{3-/4-}$ ions at BLM coated GCE in 0.1 M NaCl bath solution at various concentration of MDZ

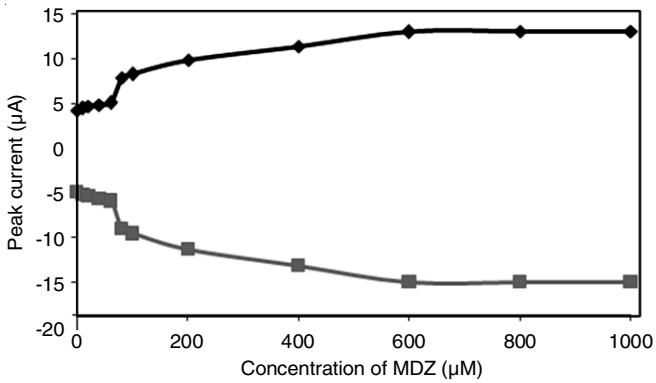

Fig. 11. Plot of redox peak currents (µA) *vs.* concentration of MDZ (µM) in the presence of 1:1 1 mM $Fe(CN)_6^{3-/4-}$ in 0.1 M NaCl bath solution at pH 7, scan rate 100 mV s^{-1}

currents also showed linearity with drug dose upto 600 µM from 80 µM. When the concentration midazolam increased further there is no change in peak currents.

When midazolam is partitioned into s-BLM, it might have introduced some more pores or increased the pore size for the penetration of marker ions, due to which $Fe(CN)_6^{3-/4-}$ ions can reach the GCE surface and show enhanced peak currents for electrochemical redox electron transfer reactions with drug dose. When the midazolam concentration becomes very high in the core of s-BLM, the pore formation or increase of pore size may be stopped due to which the peak currents in the cyclic voltammograms become almost constant with further increase in midazolam concentration beyond 600 µM. Thus, using $Fe(CN)_6^{3-/4-}$ marker ions midazolam can be detected in solutions upto 600 µM.

Conclusion

Bilayer lipid membrane (BLM) was successfully formed on the electrochemically activated GCE surface in NaCl bath solutions. The concentration of NaCl affects the membrane capacitance (C_M) and membrane resistance (R_M). With decrease in NaCl concentration in the bath solution the membrane capacitance and membrane resistance decreases. An opposite trend was observed in membrane resistance in the presence of ferri/ferrocyanide marker ions. Cyclic voltammetric studies show midazolam can be detected in solution upto 600 µM using ferri/ferrocyanide marker ions.

CONFLICT OF INTEREST

The authors declare that there is no conflict of interests regarding the publication of this article.

REFERENCES

1. A.-N. Bondar, *Chem. Rev.*, **119**, 5535 (2019); https://doi.org/10.1021/acs.chemrev.9b00093
2. L.K. Tamm and H.M. McConnell, *Biophys. J.*, **47**, 105 (1985); https://doi.org/10.1016/S0006-3495(85)83882-0
3. J.N. Robinson and D.J. Cole-Hamilton, *Chem. Soc. Rev.*, **20**, 49 (1991); https://doi.org/10.1039/cs9912000049
4. V.F. Antonov, Y.G. Rovin and L.T. Trofimov, A Bibliography of Bilayer Lipid Membranes, All Union Institute for Scientific and Technical Information, Moscow (1979).
5. A. Ulman, An Introduction to Ultrathin Organic Films: From Langmuir Blodgett to Self-Assembly, Academic Press, Boston (1991).
6. E. Sackmann, *Science*, **271**, 43 (1996); https://doi.org/10.1126/science.271.5245.43
7. P. Sondhi, D. Lingden and K.J. Stine, *Coatings*, **10**, 981 (2020); https://doi.org/10.3390/coatings10100981
8. W.M. Huang, Z.L. Zhang, X.J. Han, J.G. Wang, J.L. Tang, S.J. Dong and E.K. Wang, *Biophys. Chem.*, **99**, 271 (2002); https://doi.org/10.1016/S0301-4622(02)00227-2
9. W.M. Huang, Z.L. Zhang, X.J. Han, J.L. Tang, J.G. Wang, S.J. Dong and E.K. Wang, *Biophys. J.*, **83**, 3245 (2002); https://doi.org/10.1016/S0006-3495(02)75326-5
10. R. Pignatello, T. Musumeci, L. Basile, C. Carbone and G. Puglisi, *J. Pharm. Bioallied Sci*., **3**, 4 (2011); https://doi.org/10.4103/0975-7406.76461
11. D.A. Garcia and M.A. Perillo, *Biochim. Biophys. Acta*, **1418**, 221 (1999); https://doi.org/10.1016/S0005-2736(99)00040-1
12. B. So derpalm, *Acta Psychiatr. Scand.*, **76(Suppl.355)**, 39 (1987).
13. R. Jain and R.K. Yadav, *J. Pharm. Anal.*, **2**, 123 (2012); https://doi.org/10.1016/j.jpha.2011.11.008
14. I.L. Martin, *Neuropharmacology*, **26**, 957 (1987); https://doi.org/10.1016/0028-3908(87)90074-8
15. F.A. Stephenson, *Biochem. J.*, **249**, 21 (1988); https://doi.org/10.1042/bj2490021
16. M. Gavish, Y. Katz, S. Bar-Ami and R. Weizman, *J. Neurochem.*, **58**, 1589 (1992); https://doi.org/10.1111/j.1471-4159.1992.tb10030.x
17. R.M. Arendt, D.J. Greenblatt, D.C. Liebisch, M.D. Luu and S.M. Paul, *Psychopharmacology*, **93**, 72 (1987); https://doi.org/10.1007/BF02439589
18. M.A. Perillo and A. Arce, *J. Neurosci. Methods*, **36**, 203 (1991); https://doi.org/10.1016/0165-0270(91)90046-3
19. T. Mennini, A. Ceci, S. Caccia, S. Garattini, P. Masturzo and M. Salmona, *FEBS Lett.*, **173**, 255 (1984); https://doi.org/10.1016/0014-5793(84)81058-3
20. H. Kurishingal, P.F. Brain and C.J. Restall, *Biochem. Soc. Trans.*, **20**, 157S (1992); https://doi.org/10.1042/bst020157s
21. M.A. Perillo, L.V. Nogueira and S. Schreier, Spin Label Study of Flunitrazepam-Membrane Interaction, III Congreso Iberoamericano de Biofisica, Buenos Aires, Argentina (1997).
22. A.V. Delgado-Escueta, C. Wasterlain, D.M. Treiman and R.J. Porter, *N. Engl. J. Med.*, **306**, 1337 (1982); https://doi.org/10.1056/NEJM198206033062205
23. W. Ling and D.R. Wesson, in Eds.: D.E Smith and D.R. Wesson, The Benzodiazepines, Current Standards for Medical Practice, MTP Press, Hingham, MA, pp. 149-157 (1985).
24. R.J. DeLorenzo, S. Burdette and J. Holderness, *Science*, **213**, 546 (1981); https://doi.org/10.1126/science.6264605
25. N.C. Taft and R.J. DeLorenzo, *Proc. Natl. Acad. Sci. USA*, **81**, 3118 (1984); https://doi.org/10.1073/pnas.81.10.3118
26. J.A. Ferrendelli and S. Daniels-McQueen, *J. Pharmacol. Exp. Ther.*, **229**, 29 (1982).
27. S. Kir, A.N. Onar and A. Temizer, *Anal. Chim. Acta*, **229**, 145 (1990); https://doi.org/10.1016/S0003-2670(00)85120-X
28. C. dos Santos, V. Famila and S. Gonçalves, *Anal. Bioanal. Chem.*, **374**, 1074 (2002); https://doi.org/10.1007/s00216-002-1535-0
29. J.C. Vire, G.J. Patriarche and B.G. Hermosa, *Anal. Chim. Acta*, **196**, 205 (1987); https://doi.org/10.1016/S0003-2670(00)83085-8
30. B. Devadas, M. Rajkumar and S.-M. Chen, *Int. J. Electrochem. Sci.*, **8**, 5241 (2013).
31. D.J. Greenblatt, R.M. Arendt, D.R. Abernethy, H.G. Giles, E.M. Sellers and R.I. Shader, *Br. J. Anaesth.*, **55**, 985 (1983); https://doi.org/10.1093/bja/55.10.985
32. M. Kates, Techniques of Lipidology-Isolation, Analysis and Identification of Lipids, North-Holland Publishing Company: Amsterdam (1972).
33. N.S. Radin and J.M. Lowenste, Methods in Enzymology, Academic Press: New York (1969).
34. L.A. Geddes, Electrodes and the Measurement of Bioelectric Events, Wiley Interscience (1972).
35. A.K. Corvington, Ion-Selective Electrode Methodology, CRC Press, Boca Raton: FL, USA (1979).
36. G. Ilangovan and K.C. Pillai, *J. Solid State Electrochem.*, **3**, 357 (1999); https://doi.org/10.1007/s100080050167
37. X. Liu, W. Huang and E. Wang, *J. Electroanal. Chem.*, **577**, 349 (2005); https://doi.org/10.1016/j.jelechem.2004.12.010
38. K. Mallaiya, S. Rameshkumar, S.S. Subramanian, S. Ramalingam and T. Ramachandran, *Electrochim. Acta*, **138**, 360 (2014); https://doi.org/10.1016/j.electacta.2014.06.038
39. N. Eliaz, Applications of Electrochemistry and Nanotechnology in Biology and Medicine I, Springer Science & Business Media, vol. 52 (2011).
40. G. Favero, A. D'Annibale, L. Campanella, R. Santucci and T. Ferri, *Anal. Chim. Acta*, **460**, 23 (2002); https://doi.org/10.1016/S0003-2670(02)00139-3
41. X. Lu and T. Liao, *Int. J. Electrochem. Sci.*, **3**, 797 (2008).
42. W. Romer and C. Steinem, *Biophys. J.*, **86**, 955 (2004); https://doi.org/10.1016/S0006-3495(04)74171-5
43. J. Kotyñska and Z.A. Figaszewski, *Biomembranes*, **1720**, 22 (2005); https://doi.org/10.1016/j.bbamem.2005.11.008
44. L. Movileanu, I. Neagoe and M.L. Flonta, *Int. J. Pharm.*, **205**, 135 (2000); https://doi.org/10.1016/S0378-5173(00)00503-2
45. V. Lavaert, M. De Cock, M. Moors and E. Wettinck, *Prog. Org. Coat.*, **38**, 213 (2000); https://doi.org/10.1016/S0300-9440(00)00107-7
46. W.M. Huang, X.J. Han and E.K. Wang, *J. Electrochem. Soc.*, **150**, E218 (2003); https://doi.org/10.1149/1.1554920
47. L. Dua, X. Liu, W. Huang and E. Wang, *Electrochim. Acta*, **51**, 5754 (2006); https://doi.org/10.1016/j.electacta.2006.03.009
48. J.-S. Ye, A. Ottova, H.T. Tien and F.-S. Sheu, *Bioelectrochem.*, **59**, 65 (2003); https://doi.org/10.1016/S1567-5394(03)00003-3
49. J.O.M. Bockris, A.K.N. Reddy and M. Gamboa-Aldeco, Modern Electrochemistry: Ionics, Plenum Press (1998).